Dynamics of magnetic assembly of binary colloidal structures

F. Nogueras-Lara, L. Rodríguez-Arco and M. T. López-López

Department of Applied Physics, Campus de Fuentenueva, University of Granada, 18071, Granada, Spain

PACS 75.75.Jn – Dynamics of magnetic nanoparticles
PACS 81.16.Dn – Self-assembly
PACS 82.70.Dd – Colloids

Abstract – Magnetic field (MF)-directed assembly of colloidal particles provides a step towards the bottom-up manufacturing of smart materials whose properties can be precisely modulated by noncontact forces. Here, we study the MF-directed assembly in binary colloids made up of strong ferromagnetic and diamagnetic microparticles dispersed in ferrofluids. We present observations of the aggregation of pairs and small groups of particles to build equilibrium assemblies. We also develop a theoretical model capable of solving the aggregation dynamics and predicting the particle trajectories, a key factor to understand the physics governing the MF-directed assembly.

Introduction. – Self-assembly (SA) has been defined as "the autonomous organization of components into patterns or structures without human intervention" [1]. SA of complex structures out of simple colloidal particles is of practical interest for the fabrication of functional materials [2–13]. Furthermore, it is of fundamental interest because it represents an ideal model system in condensed matter physics for the understanding of other SA processes occurring from molecular to macroscopic length scales [1, 4, 11, 14]. We can induce or affect assembly by choosing and controlling the starting conditions or by actuating via force fields that may direct it [13, 15]. One example is the directed assembly (DA) of colloidal matter by a magnetic field (MF), which is referred to as MF-induced (or directed) assembly, or simply as magnetic assembly. Application of a MF represents a unique route to DA due to the instantaneous and anisotropic nature of magnetic interactions, as well as the reversibility that is quickly achieved by switching off the field. Another relevant advantage of magnetic assembly with respect to other routes of DA is the noncontact physical nature of magnetic interactions that enables contactless manipulation. Recent reviews on MF assembly are given in Refs. [12, 15–17].

MFs have been employed to manipulate magnetic particles and, thus, induce the formation of one-dimensional chains, two-dimensional arrays and three-dimensional assemblies [12, 15, 18–21]. Furthermore, if magnetic particles are dispersed at interfaces (liquid-liquid, air-liquid) it is possible to generate out-of-equilibrium interface assemblies able to self-propel by the application of adequate time-dependent MFs [16]. On the other hand, the response of nonmagnetic materials to applied MFs is typically so weak that it can be neglected. Nevertheless, there are some strategies to effectively manipulate nonmagnetic microparticles by MFs, such as coating them by magnetic materials (i.e., magnetic labeling) [22–24], or dispersing them in ferrofluids (FFs) [25, 26]. This latter approach enables simultaneous MF manipulation of magnetic and nonmagnetic microparticles, and has previously been used for the assembly of diamagnetic (DM) and paramagnetic microparticles into multi-component colloidal superstructures, as well as crystalline phases and fractal aggregates [4, 27–31].

In this letter, we show highly reproducible binary assemblies of strong ferromagnetic (FM) and DM microparticles occurring in FFs upon MF application. Strong ferromagnetic particles are more effectively magnetized than the paramagnetic particles mentioned in the previous paragraph, which can be advantageous for some engineering applications (e.g., magnetic separation, rheology of particulate systems, etc.). In contrast to previous studies of magnetic assembly, herein we focus on the dynamics of particle aggregation. With this aim, we experimentally track the paths that particles follow to arrange into equilibrium structures. Moreover, we develop a theoretical model capable of reproducing the particle trajectories.

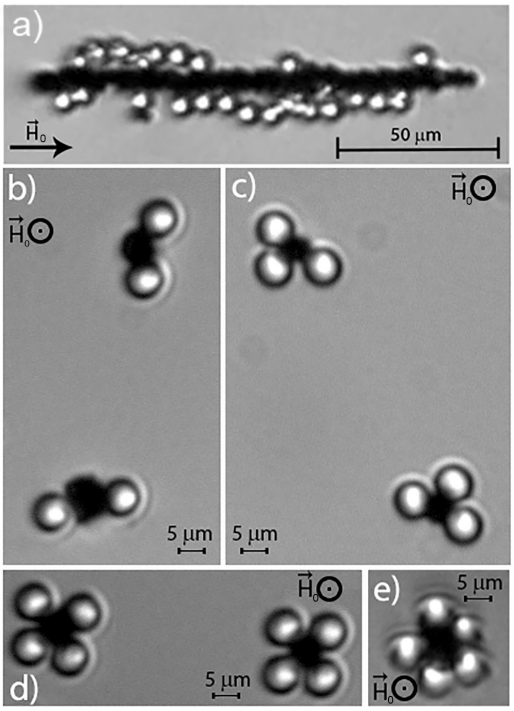

Fig. 1: Magnetic assemblies of ferromagnetic (black spheres) and diamagnetic (white spheres) microparticles in a ferrofluid (continuous medium). The applied magnetic field, $\vec{H}_0 = 10$ kAm^{-1}, was parallel to the focal plane in (a) and perpendicular to this plane in (b-e).

Experimental. – Our FFs consisted of oleate-covered magnetite nanoparticles (8.7±2.0 nm of diameter) dispersed in mineral oil with a 10 vol.% approximate particle concentration, prepared as described in Ref. [32]. As FM and DM microparticles we used Ni powder (Merck KgaA) and poly(methyl methacrylate) (PMMA) powder (Spheromers CA10, Microbeads), respectively. Mean diameter and density of the particles were 5 μm and 8.9 g cm^{-3} for Ni powder, and 6 μm and 1.2 g cm^{-3} for PMMA powder. We monitored the Ni and PMMA particle trajectories and equilibrium structures upon MF by means of an optical microscope (Thermo Fisher Scientific, USA) connected to a CCD camera. We carried out independent observations with the MF applied perpendicular or parallel to the axis of the microscope. For this purpose, we used a pair of Helmholtz coils and a single coil, respectively. The intensity of the applied MF at the focal point of the microscope was approximately homogeneous with a value of 10 kAm^{-1}, as measured with a teslameter.

Results. – Experimental equilibrium structures obtained upon MF application in diluted systems demonstrated the formation of binary assemblies of ferromagnetic (Ni) and diamagnetic (PMMA) particles (Fig. 1). Particles were assembled into anisotropic chain-like clusters oriented in the direction of the MF. These clusters mainly consisted of a central core of FM particles with some lateral chains of DM particles (Fig. 1a). Such FM-core/DM-ring configuration was better observed when the MF was applied perpendicular to the focal plane (Figs. 1b-e). In these latter experiments we observed highly reproducible flower-shaped arrangements with the FM particles acting as the core and the DM particles located at satellite positions. Similar structures were reported for non-magnetic and paramagnetic particles in FF [28] and for binary colloidal suspensions (silica and polystyrene particles) subjected to AC electric fields [33].

In order to gain understanding of the process of particle assembly, we microscopically tracked the trajectories of pairs of FM particles, pairs of DM particles and pairs of FM-DM particles (Fig. 2). As observed, for pairs of similar (either FM or DM) particles, equilibrium upon a MF was reached with the particle center-to-center line parallel to the field direction (Figs. 2d and 2i). On the other hand, for pairs of dissimilar (FM-DM) particles, the particle center-to-center line was perpendicular to the field direction in the equilibrium configuration (Fig. 2n). Remarkably, we observed the formation of some irregular dark clouds around FM microparticles when the field was connected (Figs. 2b-d and 2l-n), corresponding to regions of phase condensation of FF nanoparticles according to previous works [34, 35].

We also monitored the assembly dynamics of small groups of only a few particles (Fig. 3). As observed, when the field was connected, existing aggregates first rotated to align their axis with the direction of the external MF. Then, assembly proceeded by their aggregation with neighboring particles. Equilibrium was always reached with similar particles aligned in the direction of the applied field, and dissimilar particles aligned perpendicular to it.

Theory and discussion. – DM particles dispersed in a FF under a MF behave as magnetic hole. For each hole, an apparent magnetic moment is associated as a result of the displaced FF. This apparent moment can be approximately considered as the opposite of the total moment of the displaced FF [12, 25]. Hence, the response of a DM particle dispersed in a FF to a MF, $\vec{H}_0$, has the same nature as that of a FM particle, for which the dipole approximation of the potential energy, U_p, is [36]:

$$U_p = -2\pi a^3 \mu_f \beta_c |\vec{H}_0|^2, \qquad (1)$$

where a is the particle radius and $\beta_c = (\mu_p - \mu_f)/(\mu_p + 2\mu_f)$ the magnetic contrast factor. μ_p and μ_f are the magnetic permeabilities of the particle and the carrier fluid (i.e., the FF), respectively. Note that dipole approximation fails for systems of very close particles with β_c close to unity [36]. In these cases the effect of multipolar moments becomes relevant and cannot be neglected as it is assumed in the dipole approximation. Let us point out that β_c is considerably smaller than 1 in our case (-0.38 for PMMA particles and 0.63 for Ni particles). Note also that always $-0.5 < \beta_c < 0$ for DM particles in a FF, whereas $0 < \beta_c < 1$ for FM particles. Then, according to

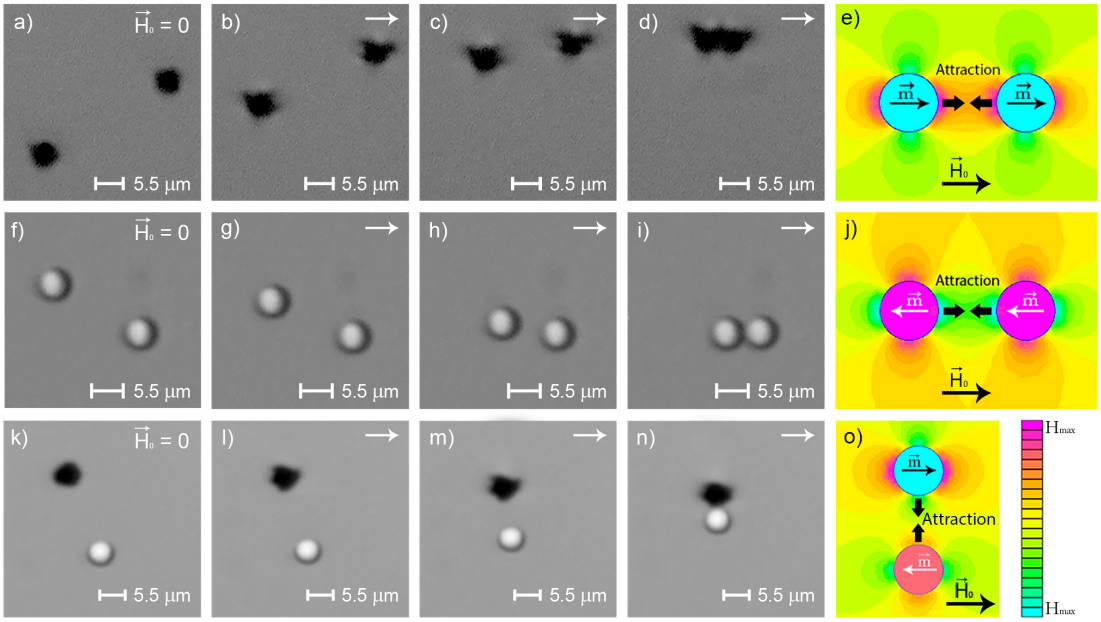

Fig. 2: Snapshots illustrating the dynamics upon a magnetic field, $\vec{H}_0 = 10$ kAm^{-1}, of pairs of microparticles dispersed in a ferrofluid (continuum medium): (a-d) two ferromagnetic particles, (f-i) two diamagnetic particles, (k-n) a ferromagnetic particle (black sphere) and a diamagnetic particle (white sphere). (a,f,k) were taken before field application (zero time). The rest of snapshots were taken at increasing times after field application. (e,j,o) show the magnetic field distribution simulated by FEM within and around ferromagnetic microparticles (blue spheres) and diamagnetic microparticles (pink spheres) dispersed in a ferrofluid, upon the application of a magnetic field, $\vec{H}_0$. The direction of the magnetic moment of the particles, $\vec{m}$, is indicated.

eq. (1), $U_p < 0$ for FM particles and, thus, they move in the direction of the MF gradient vector, towards regions of maximal MF strengths. On the contrary, $U_p > 0$ for magnetic holes, which drives them in the opposite direction of the magnetic field gradient vector towards regions of minimal MF strengths.

We solved Maxwell's equations by finite element method (FEM) and, thus, we obtained the MF distribution within and around FM and DM particles dispersed in a FF, upon a MF of constant intensity $\vec{H}_0$ (Fig. 3). For this, we assumed perfectly spherical and homogenous particles (of pure Ni or PMMA) and a continuous FF from the magnetic viewpoint. Simulations demonstrate that the MF is minimal at the equator of FM particles and at the poles of DM particles - note that equator and poles are considered with respect to the field direction. Inversely, the MF is maximal at the poles of FM particles and at the equator of DM particles. These results imply that upon MF application, FM particles move towards the poles of other FM particles and the equator of DM particles. Likewise, DM particles displace towards the poles of other DM particles and the equator of FM particles. This simple reasoning explains the positions of the particles in the equilibrium assemblies observed experimentally.

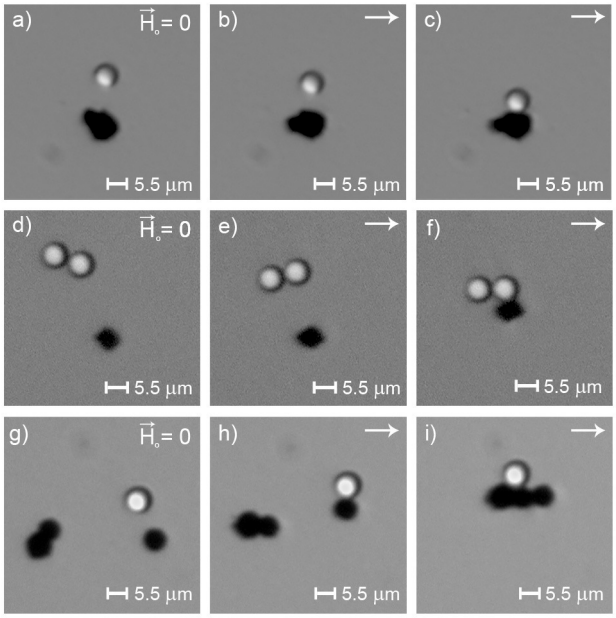

Fig. 3: Snapshots illustrating the dynamics upon a magnetic field, $\vec{H}_0 = 10$ kAm^{-1}, of small groups of ferromagnetic microparticles (black spheres) and diamagnetic microparticles (white spheres) dispersed in a ferrofluid (continuum medium). Each row corresponds to a group of particles. The first snapshot of each row was taken before field application (zero time). The rest were taken at increasing times after field application.

Let us now analyze quantitatively the process of aggregation of particles upon field application. For this purpose, we computed the theoretical trajectories by assuming the dipole approximation for the magnetostatic interaction. The most general case of a N-particle system requires 3N coordinates. However, for the sake of simplicity we assume here that all the particles and the MF vector are within the same plane, which makes the problem less cumbersome. In addition, observations of magnetic assembly are usually conducted in a single plane. In this case, the problem can be solved using polar coordinates with the origin at the center of mass of the N-particle system.

Considering two particles α, β with position vectors $\vec{r}_{\alpha,\beta}$ and magnetic dipole moments $\vec{m}_{\alpha,\beta}$. Then, under the dipole approximation, the magnetic interaction energy, $U_{\alpha\beta}$, between the two particles upon a MF, can be written as:

{

$$U_{\alpha\beta} = \frac{A_{\alpha\beta}(3cos^2\theta_{\alpha\beta} - 1)}{r^3_{\alpha\beta}}, \tag{2}$$

where $A_{\alpha\beta} = 4\pi\mu_f m_\alpha m_\beta$, $r_{\alpha\beta} = |\vec{r}_\alpha - \vec{r}_\beta| = [r^2_\alpha + r^2_\beta - 2r_\alpha r_\beta cos\theta_{\alpha\beta}]^{1/2}$, and $\theta_{\alpha\beta} = \theta_\alpha - \theta_\beta$, with θ_i the angle by which $\vec{r}_i$ is deviated from the direction of the applied MF. Consequently for a system of N-particles the Lagrangian, $\mathcal{L}$, of the system is writen as:

$$\mathcal{L} = \sum_\alpha T_\alpha - \sum_{\alpha<\beta} U_{\alpha\beta} = \sum_\alpha \frac{1}{2} m_\alpha(\dot{r}^2_\alpha + r^2_\alpha\dot{\theta}^2_\alpha) + \sum_{\alpha<\beta} \frac{A_{\alpha\beta}(3cos^2\theta_{\alpha\beta} - 1)}{r^3_{\alpha\beta}}, \tag{3}$$

with {T_α being the kinetic energy {of particle α. Note that according to estimations the absolute value of the energy given by eq. (2) for close particles is much higher than the thermal energy, $U_{Br} = kT$ (k being the Boltzmann constant and T the absolute temperature) - e.g., for particles in contact the quotient $U_{\alpha\beta}/U_{Br}$ is of the order of 10^7 for Ni-PMMA and PMMA-PMMA particles, and 10^8 for Ni-Ni particles. Thus, thermal fluctuation is negligible in our system. Particles in motion embedded in a fluid are also subjected to the friction force due to the hydrodynamic drag of the surrounding liquid. {For a spherical particle immersed in a fluid of viscosity η, this friction force, $\vec{f}_{r_\alpha}$, can be estimated by Stokes drag law:

$$\vec{f}_{r_\alpha} = -6\pi a_\alpha \eta \vec{v}_\alpha, \tag{4}$$

{where a_α and $\vec{v}_\alpha$ are, respectively, the radius and velocity of particle α. Stokes drag law makes some assumptions, mainly laminar flow and negligible hydrodynamic interactions between particles. Estimations show that the particle Reynolds number is much less than 1 ($\approx 10^{-6}$) in our experimental system and thus, the flow is laminar. Concerning hydrodynamic interactions between particles, they arise when two or more particles are close enough so that the drag on each particle is influenced by the others, and they are usually neglected for dilute systems [37].

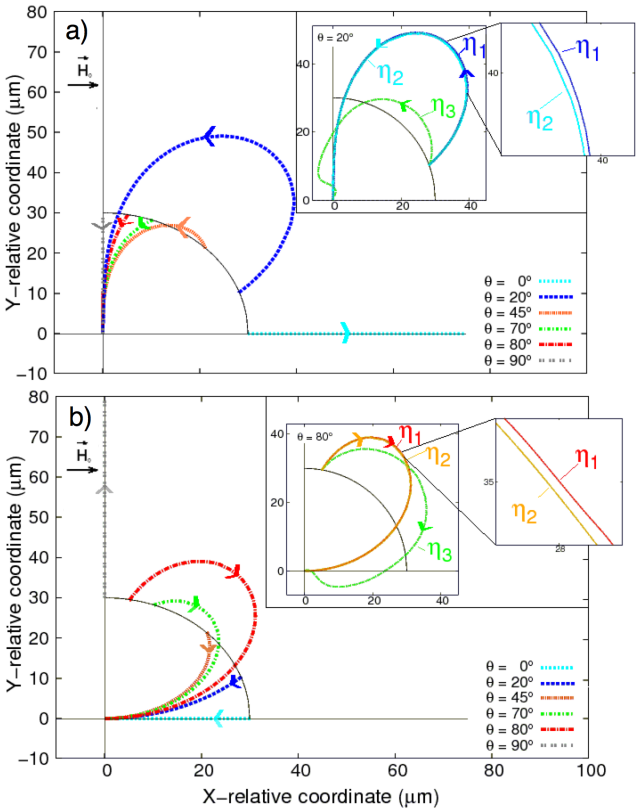

Fig. 4: Trajectories obtained by solving the equations of motion - eqs. (7) - for pairs of microparticles dispersed in a ferrofluid (viscosity 0.04 Pa·s) upon application of a magnetic field, $\vec{H}_0 = 10$ kAm^{-1}, in the direction of the x-axis. Discontinuous lines represent the trajectories of the center of one particle with respect to the center of the other particle within the particle pair. The continuous black curve represents the arc of a circumference of 30 microns of radius, which is chosen as the initial distance between the centers of the particles in all cases. The initial angle between the center-to-center line and the direction of the applied field is indicated. Trajectories are computed for pairs of similar (a) and dissimilar (b) particles. Insets depict the effect of friction by presenting theoretical calculations for different values of the carrier viscosity ($\eta_1 = 0.04$ Pa·s; $\eta_2 = 0.001$ Pa·s; $\eta_3 = 0$) and initial angle of: (a) 80°, (b) 20°.

The friction force given by eq. (4) can be introduced in our Lagrangian formulation by means of a Rayleigh dissipation function given by:

$$D_\alpha = 3\pi a_\alpha \eta(\dot{r}^2_\alpha + r^2_\alpha\dot{\theta}^2_\alpha), \tag{5}$$

where $\dot{r}_\alpha = \frac{dr_\alpha}{dt}$ and $\dot{\theta}_\alpha = \frac{dr_\alpha}{dt}$ are respectively the radial and angular velocities of particle α. Finally, the Lagrange's equations of motion can be written as:

$$M_\alpha(\ddot{r}_\alpha - r_\alpha\dot{\theta}_\alpha^2)+ \sum_{\beta>\alpha}\frac{3A_{\alpha\beta}(1-3cos^2\theta_{\alpha\beta})(r_\alpha - r_\beta cos\theta_{\alpha\beta})}{r_{\alpha\beta}^5} + k_\alpha\dot{r}_\alpha = 0 \qquad (6a)$$

$$M_\alpha r_\alpha(2\dot{r}_\alpha\dot{\theta}_\alpha + r_\alpha\ddot{\theta}_\alpha) - \sum_{\beta>\alpha}\frac{3A_{\alpha\beta}sin(2\theta_{\alpha\beta})}{r_{\alpha\beta}^3} - \frac{3A_{\alpha\beta}(1-3cos^2\theta_{\alpha\beta})(r_\alpha r_\beta sin\theta_{\alpha\beta})}{r_{\alpha\beta}^5} + k_\alpha r_\alpha^2\dot{\theta}_\alpha = 0 \qquad (6b)$$

where M_α is the mass of particle α; $\ddot{r}_\alpha = \frac{d^2r_\alpha}{dt^2}$ and $\ddot{\theta}_\alpha = \frac{d^2\theta_\alpha}{dt^2}$ are respectively its radial and angular accelerations $\{\alpha$. Let us mention that, in the simplest case of only two particles, this general problem can be reduced to a one-body problem, for which the Lagrange's equations are:

$$\mu\ddot{r} - \mu r\dot{\theta}^2 + \frac{3A}{r^4} - \frac{9Acos^2\theta}{r^4} + 6\pi a\eta\dot{r} = 0 \qquad (7a)$$

$$\mu r^2\ddot{\theta} - 2\mu r\dot{r}\dot{\theta} - \frac{6Acos\theta sin\theta}{r^3} + 6\pi a\eta r^2\dot{\theta} = 0 \qquad (7b)$$

Here, a polar coordinate system is also used, with $\vec{r}$ the position vector of the center of one of the particles with respect to the center of the other, θ is the angle by which $\vec{r}$ is deviated from the direction of the applied MF and μ the reduced mass of the 2-particle system.

The coupled systems of differential equations given by either eqs. (6) or eqs. (7) do not have analytical solution, but we can solve them numerically to obtain the particle trajectories. For this, the values of mass and magnetic moment of each of the particles and the viscosity of the carrier FF are needed. We obtained the mass by simple calculation based on the volume and the material density of the particle. For the viscosity of the FF we used the value measured (0.04 Pa·s) by using a Haake Mars III rheometer (Thermo Fisher Scientific, USA). With respect to the magnetic moment, we considered the effective dipole moment, $\vec{m}_\alpha = \beta_c a_\alpha^3\vec{H}_0$, of the particle in the applied magnetic field $\vec{H}_0$ -i.e., we neglected the effect of neighbor particles on the value of the dipole moment which gives rise to a non-negligible error when particles are close enough [36]. Note finally that our model does not have any adjustable parameter.

Fig. 4 shows trajectories for pairs of particles computed by eqs. (7). For similar particles initially aligned with the applied field (i.e., θ=0°), the trajectory is a straight line that gives rise to aggregation. As the angle of the initial center-to-center line with respect to the applied field increases, trajectories become increasingly curled. Interestingly, there is a critical angle (i.e., θ_{crit}=55°) above which particles are initially repelled increasing their relative distance, although the curled trajectories always end with aggregation of the particles. The only exception is when particles are initially aligned perpendicularly to the applied field (i.e., θ=90°). In this situation, particles are continuously repelled following a straight line.

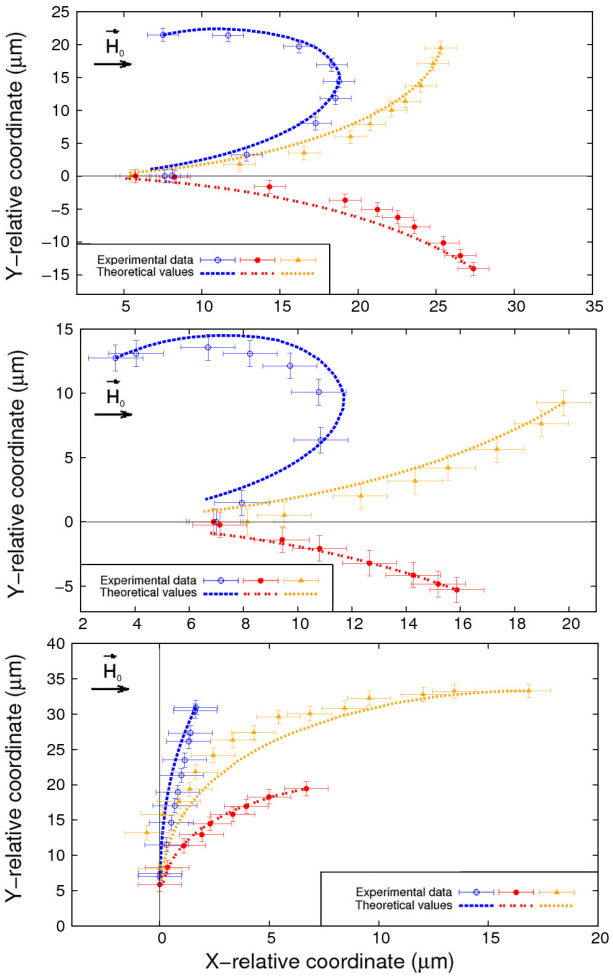

Fig. 5: Comparison of theoretical and experimental trajectories for pairs of particles dispersed in a ferrofluid (viscosity 0.04 Pa·s) upon application of a magnetic field, $\vec{H}_0$=10 kAm^{-1}, in the direction of the x-axis. Origin of the coordinate system is taken at the center of one of the particles. (a) Trajectories for 3 different pairs of Ni-Ni particles. (b) Trajectories for 3 different pairs of PMMA-PMMA particles. (c) Trajectories for 3 different pairs of Ni-PMMA particles. The final positions represent contact between particles (equilibrium position).

For dissimilar particles, the behavior is opposite: particles attract to each other following a straight line when they are initially aligned perpendicularly to the field, and repel following a line when they are initially aligned in the field direction. For initial configurations between these two limits, trajectories for particle aggregation are curled, and there is also a critical angle (i.e., θ_{crit} = 55°) below which particles are initially repelled. Concerning the effect of friction (insets of Fig. 4) we observe that in the absence of friction the trajectories are initially straighter than when friction is present, whereas they show a loop as the particles approach contact. On the other hand, in the presence of friction the trajectories show a more opened shape with a well define curvature, although there is not

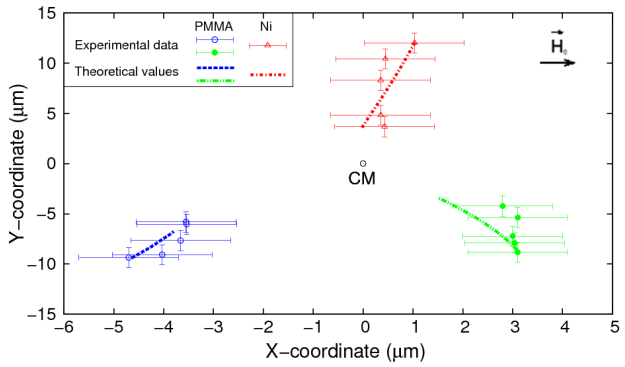

Fig. 6: Comparison of theoretical and experimental trajectories for a 3-particle system (1 Ni and 2 PMMA particles) dispersed in a ferrofluid (viscosity 0.04 Pa·s) upon application of a magnetic field, $\vec{H}_0 = 10$ kAm^{-1}, in the direction of the x-axis. The origin of the coordinate system is taken at the center of mass (CM). The closest points to CM represent equilibrium with particles in contact.

much effect of the actual value of the viscosity.

The validity of our model can be tested by comparing its theoretical predictions with the experimental trajectories obtained from pictures like those shown in Figs. 2 and 3. For pairs of particles, there is a quite good agreement between theory and experiments (Fig. 5). Theoretical predictions for small groups of more than two particles are also reasonably good, as observed, for example, for a 3-particle group consisting of 1 Ni and 2 PMMA particles (Fig.).

Conclusions. – We have shown that magnetic assembly in binary suspensions of DM and FM particles in FFs results in columnar structures that consist of a central core of FM particles and some lateral chains of DM particles, aligned with the MF. We have demonstrated that the dynamics of aggregation in this system is well predicted by a simple model that does not have any adjustable parameter. Our model computes the magnetic dipolar interactions between particles, as well as the Stokes drag force due to the liquid carrier. A more powerful theoretical model for the dynamics of magnetic assembly will require consideration of multipolar interactions between particles, phase condensation of the FF nanoparticles around the FM microparticles, as well as hydrodynamics interactions between particles, something that we envisage for the near future. Finally, the simplicity of our model is a key factor for the bottom-up design and construction of novel magnetic materials based on the magnetic field-directed assembly of non-magnetic and ferromagnetic particles. The lateral attraction between chains of opposite particles would enable building of 2-D magnetic sheets, if these chains are somehow cross-linked. Furthermore, assembly of such sheets into 3-D structures (similar to ionic crystals) would also be possible. Our model is a first step towards the design of these materials, because it could be easily encoded and used for design and engineering purposes.

* * *

The project MINECO FIS2013-41821-R (Spain) is acknowledged for financial support.

REFERENCES

[1] Whitesides G. M. and Grzybowski B., *Science*, **295** (2002) 2418.
[2] Dinsmore A. D. *et al.*, *Science*, **298** (2002) 1006.
[3] Elghanian R. *et al.*, *Science*, **277** (1997) 1078.
[4] Erb R. M. *et al.*, *Nature*, **457** (2009) 999.
[5] Freeman R. G. *et al.*, *Science*, **1629** (1995) 1629.
[6] Redl F. X. *et al.*, *Nature*, **423** (2003) 968.
[7] Shevchenko E. V. *et al.*, *Nature*, **439** (2006) 55.
[8] Vlasov Y. A. *et al.*, *Nature*, **414** (2001) 289.
[9] Xia Y. N. *et al.*, *Adv. Mater*, **13** (2001) 409.
[10] Sun S. H. and Murray C. B., *J. Appl. Phys.*, **85** (1999) 4325.
[11] Zerrouki D. *et al.*, *Nature*, **455** (2008) 380.
[12] Wang M. *et al.*, *Mater. Today*, **16** (2013) 110.
[13] Grzelczak M. *et al.*, *ACS Nano*, **4** (2010) 3591.
[14] Manoharan V. N. *et al.*, *Science*, **301** (2003) 483.
[15] Tracy J. G. and Crawford T. M., *MRS Bull*, **38** (2013) 915.
[16] Martin J. E. and Snezhko A., *Rep. Prog. Phys.*, **76** (2013) 126601.
[17] Ferrar J. A. and Solomon M. J., *Soft Matter*, **11** (2010) 4708.
[18] Martin J.E. *et al.*, *Phys. Rev. E,* , **69** (2004) 021508.
[19] López-López M. T. *et al.*, *J. Rheol.*, **53** (2009) 115.
[20] Cutillas S. *et al.*, *Phys. Rev. E*, **57** (1998) 804.
[21] Bossis G. *et al.*, *Phys. Rev.*, **594** (2002) 201.
[22] Galindo-Gonzalez C. *et al.*, *J. Appl. Phys.*, **112** (2012) 043917.
[23] Erb R. M. *et al.*, *Soft Matter*, **8** (2012) 7604.
[24] Rodríguez-Arco L. *et al.*, *Soft Matter*, **9** (2013) 5726.
[25] Skjeltorp A. T., *PRL*, **51** (1983) 2306.
[26] He L. *et al.*, *Nano Lett.*, **10** (2010) 4708.
[27] Rodríguez-Arco L. *et al.*, *Soft Matter*, **10** (2014) 6256.
[28] Ray A. *et al.*, *Phys. Rev. E.*, **82** (2010) 031406.
[29] Byrom J. and Biswal S. L., *Soft Matter*, **9** (2013) 9167.
[30] Khalil K. S. *et al.*, *Nat. Commun*, **3** (2012) 794.
[31] Ray A. and Fischer T. M., *J. Phys. Chem. B*, **116** (2012) 8233.
[32] López-López M. T. *et al.*, *J. Colloid Interface Sci.*, **291** (2005) 144-151.
[33] Ristenpart W. D. *et al.*, *Phys. Rev. Lett.*, **90** (2003) 128303.
[34] López-López M. T. *et al.*, *Soft Matter*, **6** (2010) 4346.
[35] Magnet C. *et al.*, *Phys. Rev. E*, **86** (2012) 011404.
[36] Jones T. B., *Electromechanics of Particles* (Cambridge University Press) 1995.
[37] Larson R. G., *The Structure and Rheology of Complex Fluids* (Oxford University Press) 1999.